NASA TECHNICAL MEMORANDUM

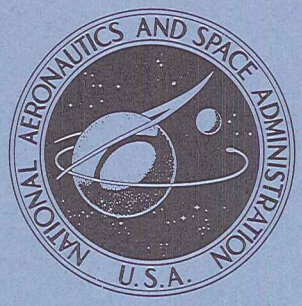

NASA TM X-2276

NASA TM X-2276

SPACECRAFT COMPONENT SURVIVABILITY DURING ENTRY INTO THE JOVIAN ATMOSPHERE

by Byron L. Swenson

Office of Advanced Research and Technology
Advanced Concepts and Missions Division
Moffett Field, Calif. 94035

NATIONAL AERONAUTICS AND SPACE ADMINISTRATION • WASHINGTON, D. C. • APRIL 1971

1. Report No.	2. Government Accession No.	3. Recipient's Catalog No.
NASA TM X-2276		

4. Title and Subtitle	5. Report Date
SPACECRAFT COMPONENT SURVIVABILITY DURING ENTRY INTO THE JOVIAN ATMOSPHERE	April 1971
	6. Performing Organization Code
7. Author(s)	8. Performing Organization Report No.
Byron L. Swenson	A-3853
	10. Work Unit No. 130-06-16-07-15
9. Performing Organization Name and Address	11. Contract or Grant No.
Office of Advanced Research and Technology Advanced Concepts and Missions Division Moffett Field, California 94035	
	13. Type of Report and Period Covered
12. Sponsoring Agency Name and Address	Technical Memorandum
National Aeronautics and Space Administration Washington, D.C. 20546	14. Sponsoring Agency Code

15. Supplementary Notes

16. Abstract

In response to the concern of the scientific community regarding the possibility of an accidental biological contamination of the middle levels of the atmosphere of Jupiter by components or fragments of an unsterilized spacecraft, an analysis has been made of the survivability of such bodies upon entry along possible entry trajectories. Survivability boundaries are calculated in terms of the body size and the material specific heat capacity and are shown for various average body specific gravities and as a function of entry angle.

17. Key Words (Suggested by Author(s))	18. Distribution Statement
Jupiter entry Biological contamination	Unclassified – Unlimited

19. Security Classif. (of this report)	20. Security Classif. (of this page)	21. No. of Pages	22. Price*
Unclassified	Unclassified	18	$3.00

*For sale by the National Technical Information Service, Springfield, Virginia 22151

SYMBOLS

A	reference area, m^2
C_c	convective constant
C_D	drag coefficient
C_r	radiative constant
H_{eff}	specific heat capacity, J/kg
K	density ratio across a normal shock, ρ_s/ρ
m	body mass, kg
P	pressure, bars
q	heating rate, W/m^2
Q	heat load, J
R	body radius, m
R_s	shock radius, m
S	surface area, m^2
t	time, sec
V	free-stream velocity, m/sec
γ_I	inertial entry angle, deg
γ_R	relative entry angle, deg
δ	local shock standoff distance, m
Δ	stagnation-point shock standoff distance, m
ρ	free-stream density, kg/m^3
σ	specific gravity
θ	body location, deg
Γ	radiation cooling parameter

Subscripts

AD	adiabatic shock layer
c	convective
n	normal component
r	radiative
s	stagnation point

SPACECRAFT COMPONENT SURVIVABILITY DURING ENTRY INTO THE JOVIAN ATMOSPHERE

Byron L. Swenson

Office of Advanced Research and Technology
Advanced Concepts and Missions Division
Moffett Field, California 94035

SUMMARY

In response to the concern of the scientific community regarding the possibility of an accidental biological contamination of the middle levels of the atmosphere of Jupiter by components or fragments of an unsterilized spacecraft, an analysis has been made of the survivability of such bodies upon entry along possible entry trajectories. Survivability boundaries are calculated in terms of the body size and the material specific heat capacity and are shown for various average body specific gravities and as a function of entry angle.

The results, in general, indicate that at a given material heat capacity, shock layer radiation heating completely destroys most large bodies or fragments while convective heating from the boundary layer completely destroys most small bodies or fragments. The degree of size overlap from these two destructive heating mechanisms depends primarily on the specific heat capacity of the body and the angle of entry and only to slight extent on the specific gravity or density of the body. It is shown that unprotected metal pieces, regardless of size and material, will not survive entry and will not penetrate even to the top of the atmospheric cloud layer. It is possible for bodies with effective specific heat capacities in excess of about 10–15 MJ/kg to survive entry but only if the body size is in the vicinity of 0.5 to 1 m in radius. Some plastics, due to the nature of their ablation characteristics, will have effective specific heat capacities in this range but pieces of this size on any planned spacecraft are doubtful except for probes, which are designed to survive and are probably sterilized.

There is, of course, a considerable uncertainty in the knowledge of the structure and composition of the atmosphere of Jupiter and in the calculation of the thermal environment for entries into that atmosphere at the extreme speeds typical of a Jupiter encounter. However, considering the magnitude of these uncertainties relative to the results of the present analysis, it appears that biological contamination of the middle levels of the atmosphere of Jupiter by an accidental impact of an unsterilized spacecraft is doubtful.

INTRODUCTION

During this and the next decade, several unmanned missions are planned, which will pass close to Jupiter. Because the middle regions of the atmosphere of Jupiter are thought to contain conditions conducive to the replication of life, considerable concern has been voiced in the

scientific community about the possibility of biological contamination of Jupiter through an accidental impact of an unsterilized spacecraft. This report is an analysis of the survivability of spacecraft components or fragments upon atmospheric entry from hyperbolic approach conditions. Its purpose is to assist in assessing the contamination danger.

ANALYSIS

Because of the massiveness of Jupiter, the inertial entry velocity resulting from typical hyperbolic approach velocities is always about 61 km/sec. Because of the very high rotation rate and the size of Jupiter, however, the entry velocity relative to the rotating atmosphere can be as low as about 50 km/sec for eastward equatorial entries at shallow entry angles. As the entry angle steepens, the relative entry velocity increases rapidly. Obviously, the dissipation of such high kinetic energies must result in immense aerodynamic heating. Such heating to the body results principally from the radiation from the high temperature, high-pressure shock layer that envelopes the body and from the frictional convective heating from the boundary layer.

Both these heating mechanisms depend on the shape or configuration of the body. Fortunately, from an analysis point of view, the effects of configuration tend to be somewhat compensating; that is, a shape with high radiative heating tends to have lower convective heating and vice versa. Since, in general, the shape of spacecraft components or fragments is not known, the simplest shape, a sphere, is assumed for this analysis. If the analysis should indicate that survivability may be a problem, then the effect of other configurations would have to be examined. In addition, it was assumed that the bodies are tumbling such that the entire mass of the body is available for heat absorption.

As stated before, an inertial entry velocity of 61 km/sec is assumed. At this speed, bodies flying along trajectories with inertial entry angles shallower than about -5° (at an altitude of 305 km above the cloud top) will skip out of the atmosphere hyperbolically and will thus escape and not present a contamination problem. Therefore entry angles steeper than -5° are of interest. Only eastward entries are of interest for this analysis since the relative entry velocity of other entry azimuths is always greater.

The atmosphere model assumed for this analysis is rather nominal compared with models in the literature (refs. 1–5). The assumed composition is 85 percent H_2 and 15 percent He. A scale height of 20.7 km is assumed, which is consistent with a 140° K stratospheric temperature.

Radiative Heating

The radiative heating from the high-temperature, high-pressure shock layer that envelopes the body for the entry conditions and the atmosphere model just discussed have been calculated by Tauber, and some of the results are presented in reference 6. The results of basic calculations of the radiative intensity behind a normal shock, assuming an adiabatic shock layer at various flight conditions, are shown in figure 1. These are unpublished calculations on which the results of reference 6 are based. In the figure, radiative intensity reaching the wall for an adiabatic shock layer of 1 cm thickness is plotted versus free-stream velocity for various values of pressure behind the

normal shock. Calculations of the effect of self-absorption of the gas in the shock layer indicate that the intensity reaching the wall varies roughly as the six-tenths power of the standoff distance.

Figure 1 can be used to form the following simple approximate relationship, in terms of free-stream velocity and density, between the size of the spherical body and the stagnation-point radiative heating rate reaching the wall for an adiabatic shock layer.

$$(q_{s,r})_{AD} = 1.24 \times 10^{-25} \rho^{1.365} V^{8.55} \left(\frac{\Delta}{R}\right)^{0.6} R^{0.6} \tag{1}$$

The parameter Δ is the stagnation-point shock standoff distance. This relationship appears to be within ±50 percent of the radiative intensity shown in figure 1 over a range of velocities from 30 to 55 km/sec and shock layer pressures from 0.1 to 10 bars.

The so-called radiative cooling effect discussed in reference 6 causes the actual radiative emission of the shock layer to be somewhat less than predicted by equation (1) for an adiabatic shock layer. Accordingly, the radiative heating rate reaching the wall for the nonadiabatic hydrogen-helium shock layer is given approximately by (ref. 6):

$$q_{r,s} = \frac{(q_{r,s})_{AD}}{1 + 3\Gamma^{0.7}}$$

where the radiation cooling parameter Γ is

$$\Gamma = \frac{2(q_{r,s})_{AD}}{1/2\rho V^3}$$

The total integrated radiative heat load received by the body during entry is the integral of the heating rate over the body surface integrated over the time of the entry trajectory

$$Q_r = \int_t \int_S q_r \, dS \, dt$$

Normalizing the heating rate, q_r, by the stagnation-point heating rate, $q_{s,r}$, and assuming that the normalized heating rate distribution is invariant with flight conditions allows the integrations to be separated, yielding

$$Q_r = \int_t q_{s,r} \, dt \int_S (q/q_s)_r \, dS \tag{2}$$

This assumption will be verified in the subsequent discussion.

The normalized distribution of radiative heating over the body can be determined approximately by applying the results of figure 1 or equation (1) using the local pressure, the local component of velocity normal to the shock, and the local shock standoff distance. It is obvious, therefore, that the shape of the shock wave is critical to this determination. It should be noted that it is assumed that radiation cooling does not affect the normalized heating rate distribution.

The shock-wave shape about a sphere in hypersonic flow is governed almost exclusively by the density ratio across the shock at the stagnation point. The results of references 7 and 8 indicate that for large density ratios across a normal shock, the standoff distance at the stagnation point of a sphere of radius R is given by

$$\frac{\Delta}{R} = \frac{0.78}{K} \tag{3}$$

where $K = \rho_s/\rho$, the density ratio across a normal shock. Tauber's results show that a density ratio of about 12 is typical for the entries of interest.

The shape of the shock wave about the body can be determined from the results of reference 8. It can be shown that the shock shape for a sphere is itself spherical up to about 60° from the stagnation point with a radius equal to the body radius plus three stagnation-point standoff distances.

$$\frac{R_s}{R} = 1 + 3\frac{\Delta}{R} \tag{4}$$

Based on equation (1) and figure 2, the radiative heating rate at a location an angle θ away from the stagnation point when normalized by the stagnation-point heating rate is given by

$$\left(\frac{q}{q_s}\right)_r = \left(\frac{p}{p_s}\right)^{1.365}\left(\frac{V_n}{V}\right)^{5.82}\left(\frac{\delta}{\Delta}\right)^{0.6}$$

Using the shock wave geometry as described by equation (4) and as shown in figure 2 and a Newtonian pressure distribution results in a normalized radiative heating distribution as shown in figure 3. Under the assumptions made, this heating distribution is invariant with respect to flight conditions. Integrating the distribution over the body surface area (to $\theta = 90°$) results in a normalized radiative heating area of:

$$\int_S (q/q_s)_r \, dS = 0.83R^2 \tag{5}$$

The integral of the stagnation-point heating rate over the time of the entry trajectory (i.e., the first integral of eq. (2)) is a function only of body ballistic parameter, m/C_DA, the entry angle, and the body radius, R. Digital machine calculations of ballistic entries at various entry angles and several ballistic coefficients for an inertial entry speed of 61.5 km/sec have been made and the calculated stagnation-point radiative heat loads for a 1 m radius spherical body are shown in figure 4. These results indicate that the stagnation-point radiative heat load calculated from equation (1) varies as $(m/C_DA)^{1.255}$ as shown on the left-hand side of the figure. The variation of stagnation-point heat load with entry angle is shown on the right-hand side of figure 4. This variation is seen to be approximately proportional to the sine of the relative entry angle to the 0.255 power for small entry angles but to deviate significantly at large entry angles because of the rapid increase in relative entry speed with increasing entry angle.

The results of figure 4 can be used to write the stagnation-point heat load as

$$\int_t q_{s,r} \, dt = C_r(\gamma_R)\left(\frac{m}{C_DA}\right)^{1.255} R^{0.6} \tag{6}$$

where $C_r(\gamma_R)$ is given in the following table.

γ_I	γ_R	C_r
-5°	-6.29°	$9.2X10^6$
-15°	-18.80°	$1.31X10^7$
-45°	-54.67°	$2.44X10^7$
-90°	-78.37°	$5.49X10^7$

Combining equations (5) and (6) yields the following expression for the total radiative heat load received by the body during entry

$$Q_r = 0.83C_r\left(\frac{m}{C_DA}\right)^{1.255} R^{2.6} \tag{7}$$

Convective Heating

As was indicated in reference 9, the stagnation-point convective heating rate in the hydrogen rich atmosphere of Jupiter is approximately 35 percent of the value at similar flight conditions in air. Therefore an adequate expression for the stagnation-point convective heating rate in terms of the free-stream velocity and density and body radius is:

$$q_{s,c} = 6.82X10^{-5}\sqrt{\rho/R}\, V^3 \tag{8}$$

The total integrated convective heat load received by the body during entry is the integral of the heating rate over the body surface integrated over the time of the entry trajectory

$$Q_c = \int_t \int_S q_c \, dS \, dt$$

Normalizing the heating rate, q_c, by the stagnation-point heating rate, $q_{s,c}$, and noting from reference 10 that the normalized distribution is essentially invariant with flight conditions allows the integrations to be separated, yielding

$$Q_c = \int_t q_{s,c} \, dt \int_S (q/q_s)_c \, dS \tag{9}$$

The integral of the normalized heating rate distribution over the surface of a sphere can be calculated from the results of reference 10. The resulting normalized convective heating area is:

$$\int_S \left(\frac{q}{q_s}\right)_c dS = 2.5R^2 \tag{10}$$

As was the case for the radiative heating, the integral of the stagnation-point heating rate over the time of the entry trajectory is a function only of the ballistic parameter, m/C_DA, the entry angle, and the body radius, R. The digital calculations of the stagnation-point convective heat loads for a 1 m radius spherical body as a function of ballistic parameter for various entry angles are shown in figure 5. The results indicate that the stagnation-point convective heat load varies as $(m/C_DA)^{0.5}$. The variation with relative entry angle as shown on the right-hand side of figure 5 is about proportional to $[\sin(\gamma_R)]^{-0.5}$. There is, however, a significant deviation from this proportionality at high entry angles again resulting from the rapid increase in relative entry speed with increasing entry angle.

The results of figure 5 can be used to write the stagnation-point heat load as

$$\int_t q_{s,c}\, dt = C_c(\gamma_R)\left(\frac{m}{C_D A}\right)^{0.5} R^{1.5} \tag{11}$$

where $C_c(\gamma_R)$ is given in the following table

γ_I	γ_R	C_r
-5°	-6.29°	1.24×10^8
-15°	-18.80°	7.45×10^7
-45°	-54.67°	5.45×10^7
-90°	-78.37°	6.89×10^7

Combining equations (10) and (11) yields the following expression for the total convective heat load received by the body during entry

$$Q_c = 2.5C_c\left(\frac{m}{C_D A}\right)^{0.5} R^{1.5} \tag{12}$$

Survivability

In order to determine the size and mass of bodies that will survive either the radiative heat load or the convective heat load, the heat absorbed for such bodies must be less than the heat capacity of those bodies. For simplicity, the heat capacity of a body is considered to be the product of the mass of the body and an effective specific heat capacity of the body material. This effective specific heat capacity includes the internal heat capacity, any phase change heats of formation or decomposition, and any heat blockage effects due to an ablation process. Therefore the minimum effective specific heat capacity for survival is determined from

$$Q < mH_{eff} \tag{13}$$

Substituting either equation (7) or equation (12) into equation (13) and using a drag coefficient, C_D, of unity based upon cross sectional area results in a relationship for survivability of:

$$m^{0.255} R^{0.09} < \frac{5.07H_{eff}}{C_r} \tag{14}$$

and

$$\left(\frac{m}{R}\right)^{1/2} > \frac{1.41C_c}{H_{eff}} \tag{15}$$

from radiative heating and convective heating, respectively. Equations (14) and (15) can be further reduced if one introduces the body average specific gravity, σ, and solves for the body radius. The result is a size condition for survival of:

$$R < \frac{(H_{eff}/C_r)^{1.17}}{1.803\sigma^{0.298}} \tag{16}$$

and

$$R > \frac{C_c}{45.9\sigma^{1/2}H_{eff}} \tag{17}$$

for radiative heating and convective heating, respectively.

It can be seen from equations (16) and (17) that at a given heat capacity, radiative heating destroys large bodies and convective heating destroys small bodies. The degree of size overlap from these two destructive heating mechanisms is a direct function of the effective specific heat capacity and the entry flight path angle (contained within the parameters C_r and C_c) and only a weak function of the body specific gravity. This dependence is shown graphically in figures 6(a) to 6(c) where these survivability boundaries are plotted in terms of body size and specific heat capacity.

Figure 6(a) shows results for an average body specific gravity of 20, which represents about the upper limit of possible body density. Solid bodies made of tungsten, platinum, or gold fall into this specific gravity category. The straight-line boundary running from the lower left-hand side to the upper right-hand side of the figure represents the survivability boundary for spherical bodies from radiative heating only for an inertial entry angle of -5°. Bodies with effective specific heat capacities less than indicated by this line will not survive. The straight-line boundary running from the upper left-hand side to the lower right-hand side of the figure represents a similar boundary for convective heating only. At a given size, then, a body with a specific heat capacity equal to the sum of the heat capacity which will just survive radiative heating plus the heat capacity which will just survive convective heating will survive the combined heat input. This survival boundary for combined radiative and convective heating is the curved boundary so indicated. The region to the right of this boundary is the survivable region. It can easily be seen that all bodies with effective specific heat capacities less than about 10 MJ/kg will not survive either because radiative heating predominates or because convective heating predominates, or both. The effect of entry angle is illustrated by the indicated dash-dot line that shows the locus of the boundary intersection points. Increasing the entry angle enhances aerothermal destruction. It is also interesting that for heat capacities greater than 10 MJ/kg there is a preferred body size for survival of the order of 10 cm in radius for this specific gravity.

The effect of body specific gravity is illustrated by figures 6(b) and 6(c) where similar results are presented for an average specific gravity of 2 and 0.2, respectively. As mentioned before, a specific gravity of 20 is typical of platinum or tungsten. Solid bodies of copper or steel have specific gravities near 10. Solid bodies of aluminum, magnesium, or beryllium have specific gravities near 2.5. Hollow bodies like spacecraft tanks have thickness-to-radius ratios of about 1:40 and thus have average specific gravities ranging from about 1 for steel to about 0.2 for aluminum. Most plastics have a specific gravity in the range of 1 to 0.5. The main effect of body specific gravity on survivability is to change the preferred body size for survival. In general, the preferred body size increases as specific gravity decreases. A preferred size of about 1 m in radius is apparent for a specific gravity of 0.2.

It is apparent that for all values of specific gravity, a minimum effective specific heat capacity of about 10 to 15 MJ/kg is required for survival. The effective specific heat capacity of most metals up to and including melting is near 1 MJ/kg. Beryllium has a very high heat capacity near 5 MJ/kg. It is apparent from the previous results, therefore, that all unprotected metal pieces will be completely destroyed regardless of size.

While the heat absorption ability of metals is connected to the internal thermal capacity and the latent heat of melting of the material, the primary heat absorption mechanism for plastics is surface ablation. The low diffusivity of plastics results in a rapid rise in the surface temperature to the vaporization or depolymerization temperature of the material. Additional heat is then absorbed in the latent heat of decomposition which produces quantities of low-molecular weight gases that transpire into the boundary layer changing the velocity and temperature profiles within that layer and further reducing the incident convective heat transfer. In addition, the ablation-produced gases also block some of the incident radiative heat transfer by absorption. Thus the effective specific heat capacities of ablation materials can be quite high. Lumping all these heat absorption effects together results in a specific heat capacity for most ablating materials in the range from about 7 to as much as 30 MJ/kg. It appears, therefore, that it is possible for ablation protected bodies to survive entry. It should be remembered, however, that the average specific gravity of such bodies is low, and thus to survive, such a body must be of the order of 0.5 to 1 m in radius.

CONCLUSIONS

Considering the magnitude of the uncertainties associated with the knowledge of atmosphere structure and compositon, the uncertainties associated with the calculation of the entry thermal environment, and the limitations of the assumptions of the present analysis, the following conclusions appear appropriate.

1. For a given material specific heat capacity, shock layer radiative heating completely destroys large bodies while convective heating from the boundary layer completely destroys small bodies.

2. The degree of size overlap from these two destructive heating mechanisms depends primarily upon the specific heat capacity of the body material and the entry flight path angle.

3. All bodies with specific heat capacities less than about 10 MJ/kg will be destroyed by either the predominate radiative heating or the predominate convective heating or both, regardless of size or the entry flight path angle.

4. A preferred size for survival exists for bodies with specific heat capacities greater than about 10 MJ/kg. This size ranges from about 10 cm radius for a body specific gravity of 20 to about 1 m radius for a body specific gravity of 0.2.

5. Since all metals have specific heat capacities less than 5 MJ/kg, all unprotected metal bodies will not survive entry regardless of size.

6. Since some plastic ablation materials will have specific heat capacities of nearly 30 MJ/kg, bodies of such materials will survive entry; however, the size of such bodies will have to be of the order of at least 0.5 m in radius.

NASA Headquarters
Moffett Field, Calif., 94035, January 21, 1971

REFERENCES

1. Gross, S. H.; and Rasool, S. I.: The Upper Atmosphere of Jupiter. Icarus, vol. 3, 1964, pp. 311–322.

2. Lewis, John S.: The Clouds of Jupiter and the NH_3–H_2O and NH_3–H_2S Systems. Icarus, vol. 10, May 1969, pp. 365–378.

3. Hogan, Joseph S.: The Thermal Structure of the Jovian Atmosphere. J. Atmos. Sci., vol. 26, no. 5, pt. 1, Sept. 1969, pp. 898–905.

4. Trafton, L. M.: Model Atmosphere of the Major Planets. Astrophys. J., vol. 147, no. 2, Feb. 1967, pp. 765–781.

5. Hunten, Donald M.: The Upper Atmosphere of Jupiter. J. Atmos. Sci., vol. 26, no. 5, pt. 1, Sept. 1969, pp. 826–834.

6. Tauber, M. E.; and Wakefield, R. M.: Heating Environment and Protection During Jupiter Entry. Presented at AIAA 7th Annual Meeting and Technical Display, Houston, Texas, Oct. 19–22, 1970. AIAA Paper 70–1324.

7. Van Dyke, M. D.: The Supersonic Blunt Body Problem – Review and Extensions. J. Aero/Space Sci., vol. 25, no. 8, Aug. 1958, pp. 485–496.

8. Edsall, Robert H.: Calculation of Flow Fields About Blunt Bodies of Revolution Traveling at Escape Velocity. Technology of Lunar Exploration, Progress in Astronautics and Aeronautics, Academic Press, Inc., New York, vol. 10, Oct. 1963, pp. 817–852.

9. Tauber, M. E.: Atmospheric Entry Into Jupiter. J. Spacecraft and Rockets, vol. 6, no. 10, Oct. 1969, pp. 1103–1109.

10. Lees, L.: Laminar Heat Transfer Over Blunt-Nosed Bodies at Hypersonic Flight Speed. Jet Propulsion, vol. 26, no. 4, April 1956, pp. 259–269.

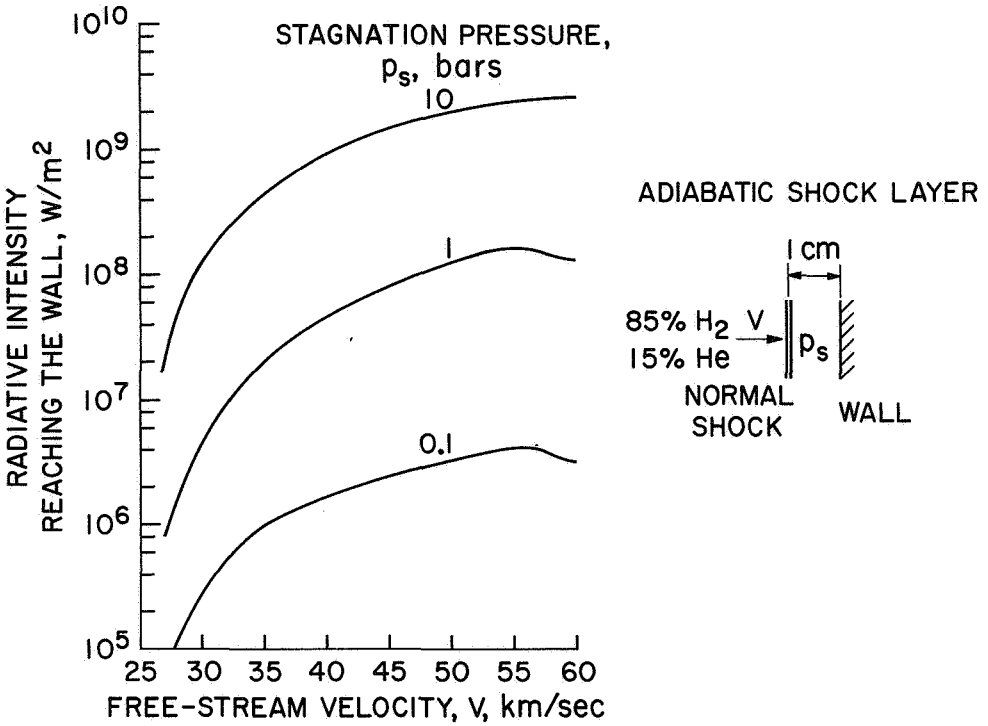

Figure 1.- Shock-layer radiative intensity for an adiabatic shock layer as a function of flight conditions.

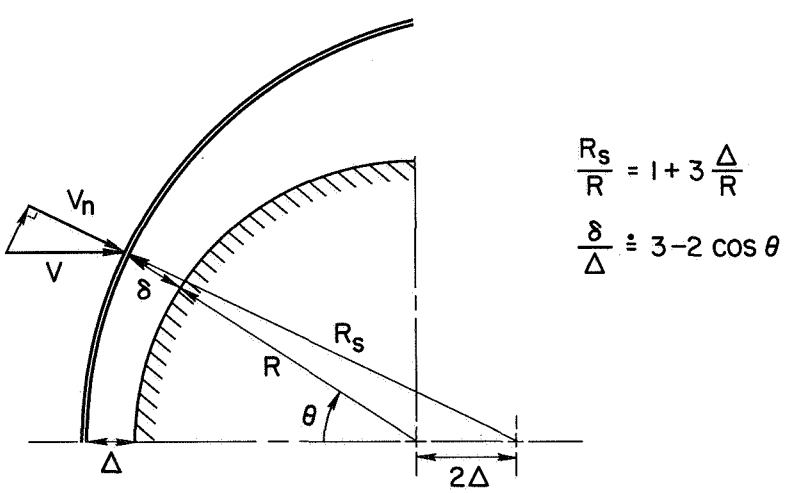

Figure 2.- Approximate shock-layer geometry about a spherical body.

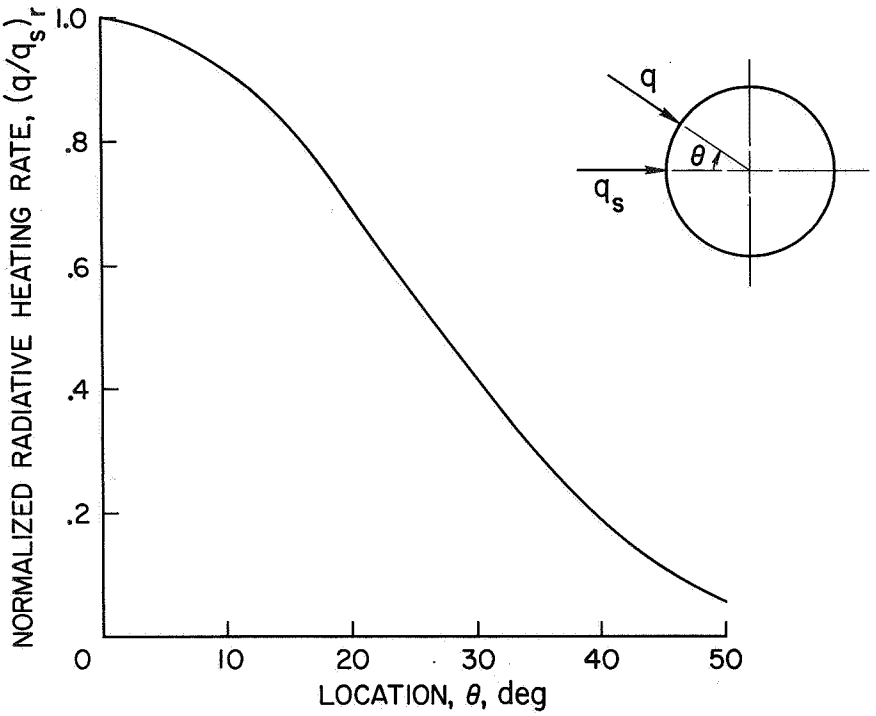

Figure 3.- Normalized radiative heating-rate distribution about a spherical body.

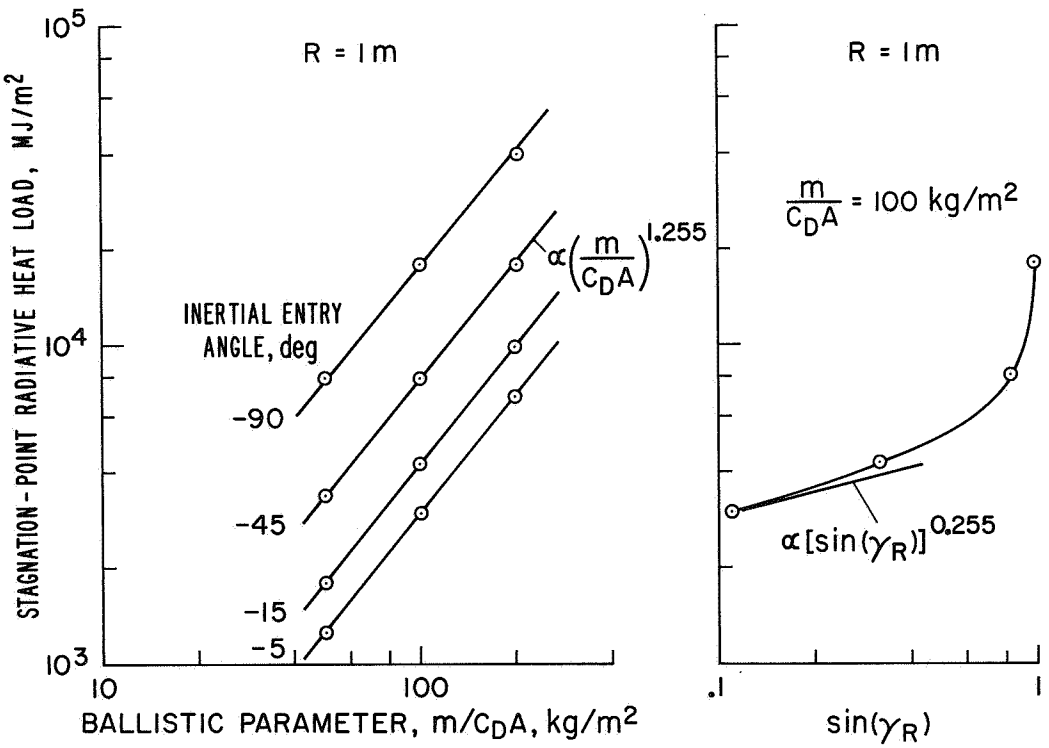

Figure 4.- Stagnation-point radiative heat loads as a function of ballistic parameter and entry angle.

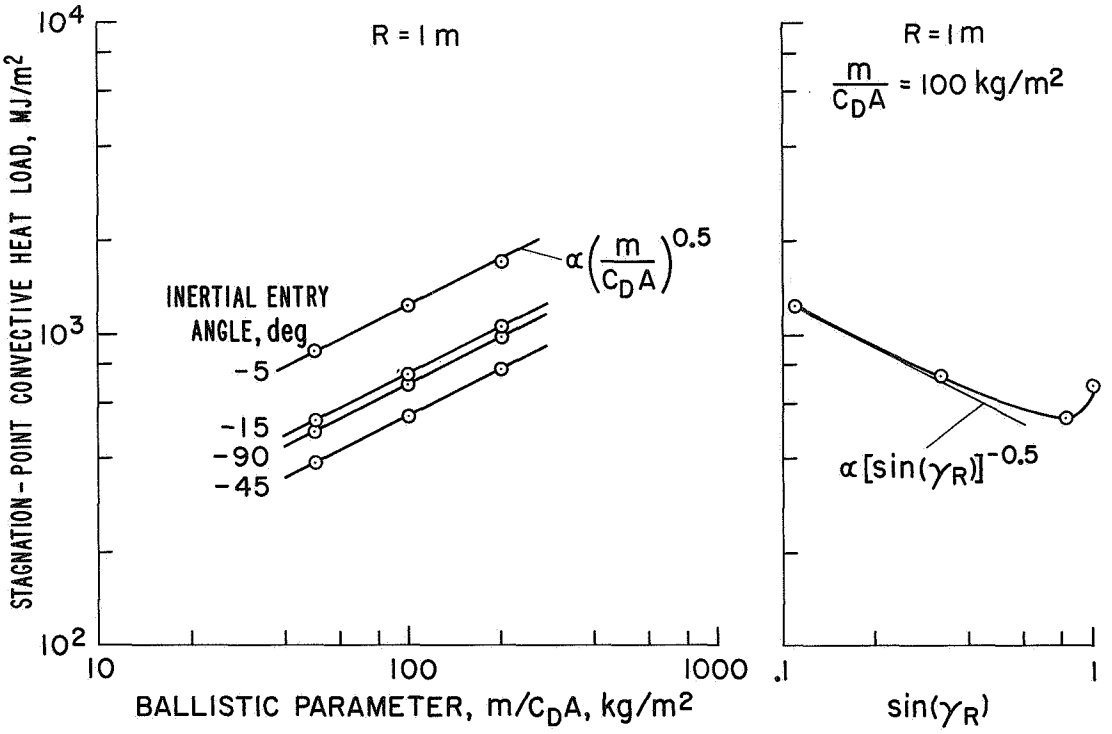

Figure 5.- Stagnation-point convective heat loads as a function of ballistic parameter and entry angle.

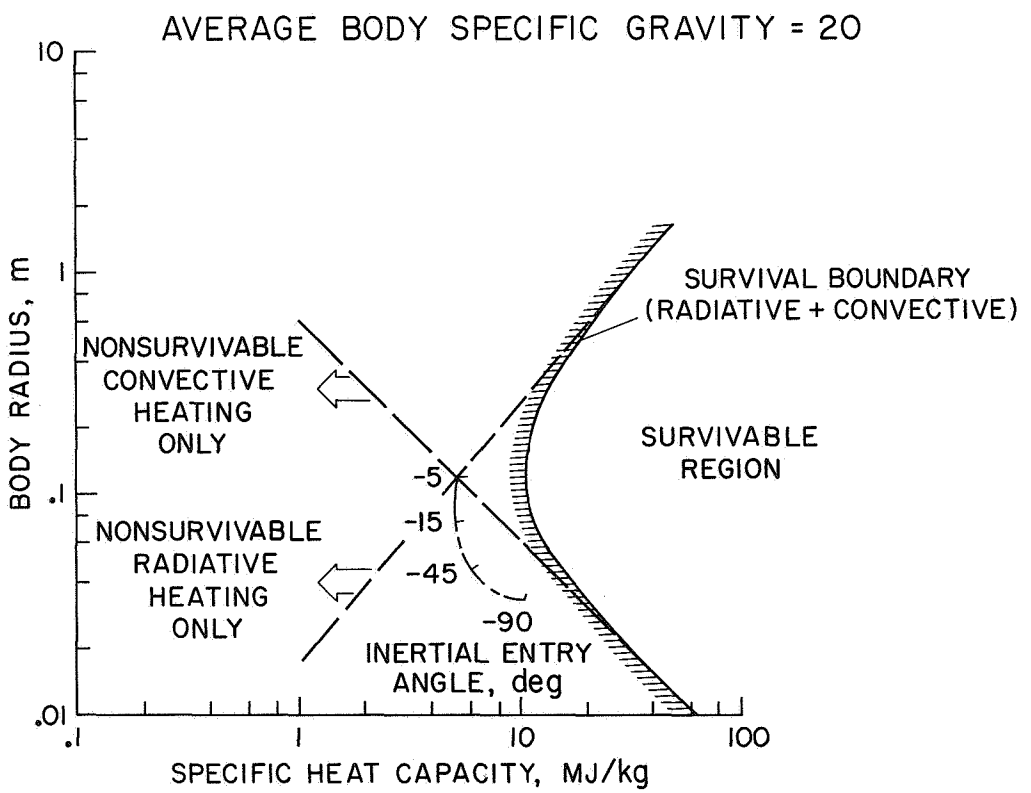

(a) $\sigma = 20$

Figure 6.- Survivability boundaries.

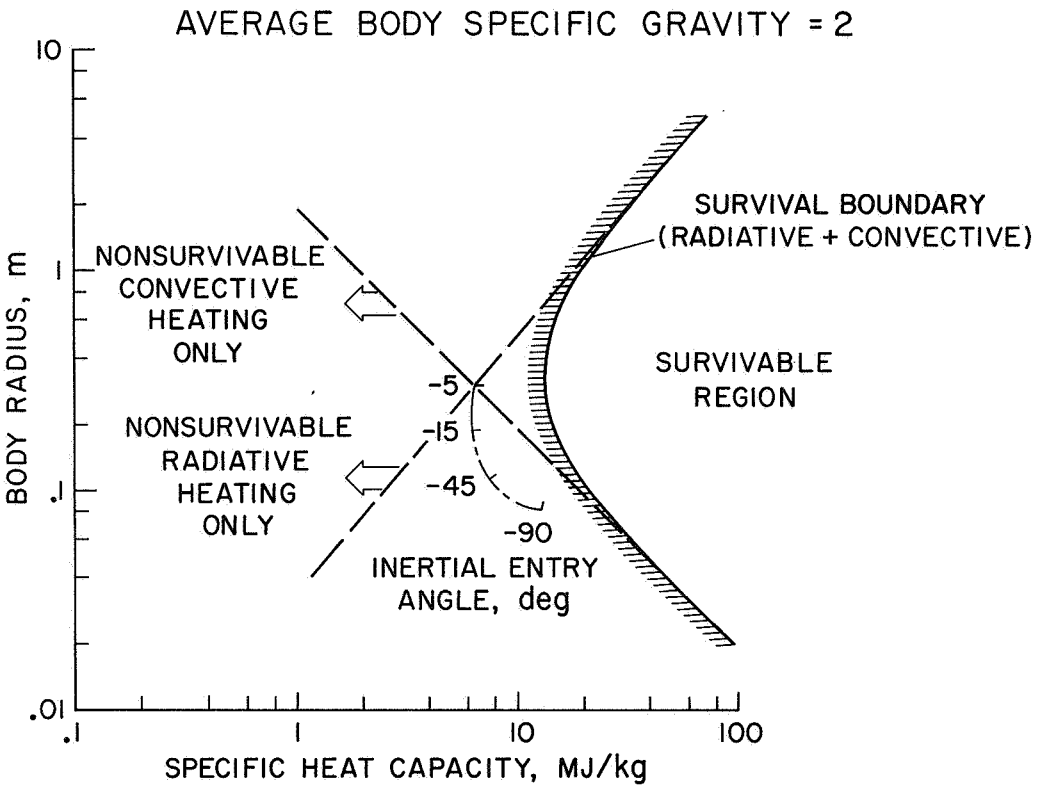

(b) $\sigma = 2$

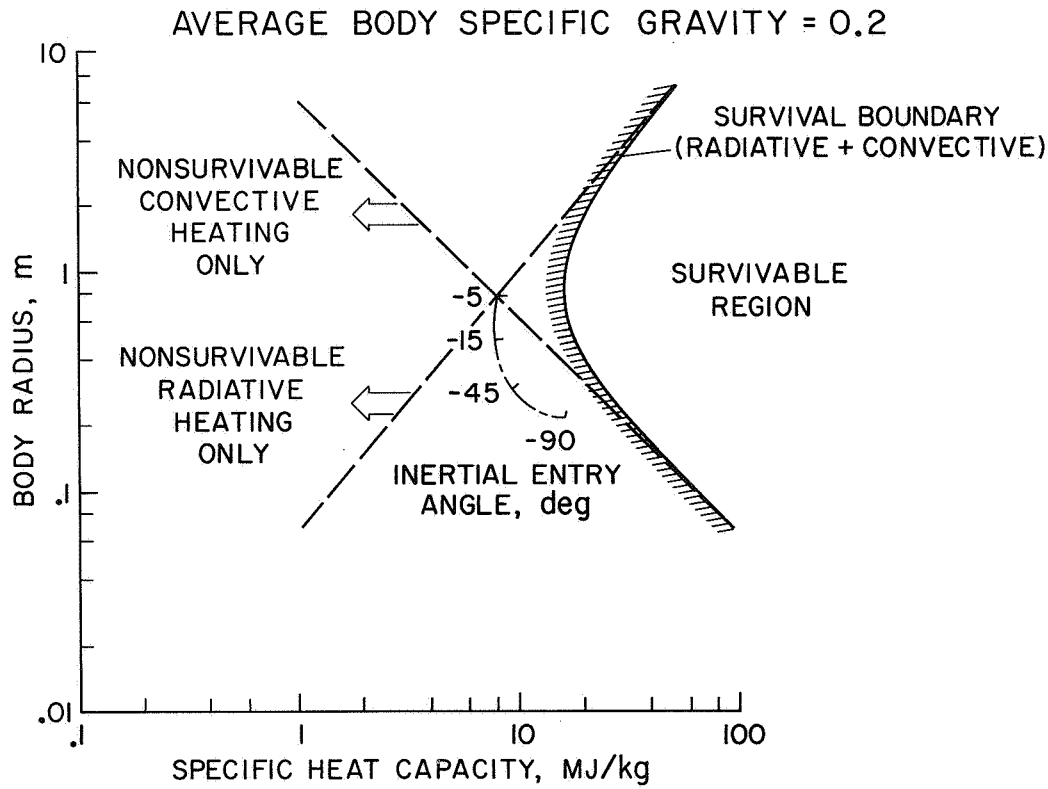

(c) $\sigma = 0.2$

Figure 6.- Concluded.

NASA-Langley, 1971 —— 4 A-3853

NATIONAL AERONAUTICS AND SPACE ADMINISTRATION
WASHINGTON, D.C. 20546

OFFICIAL BUSINESS
PENALTY FOR PRIVATE USE $300

FIRST CLASS MAIL

POSTAGE AND FEES PAID
NATIONAL AERONAUTICS AND
SPACE ADMINISTRATION

POSTMASTER: If Undeliverable (Section 158
Postal Manual) Do Not Return

"The aeronautical and space activities of the United States shall be conducted so as to contribute . . . to the expansion of human knowledge of phenomena in the atmosphere and space. The Administration shall provide for the widest practicable and appropriate dissemination of information concerning its activities and the results thereof."

—NATIONAL AERONAUTICS AND SPACE ACT OF 1958

NASA SCIENTIFIC AND TECHNICAL PUBLICATIONS

TECHNICAL REPORTS: Scientific and technical information considered important, complete, and a lasting contribution to existing knowledge.

TECHNICAL NOTES: Information less broad in scope but nevertheless of importance as a contribution to existing knowledge.

TECHNICAL MEMORANDUMS: Information receiving limited distribution because of preliminary data, security classification, or other reasons.

CONTRACTOR REPORTS: Scientific and technical information generated under a NASA contract or grant and considered an important contribution to existing knowledge.

TECHNICAL TRANSLATIONS: Information published in a foreign language considered to merit NASA distribution in English.

SPECIAL PUBLICATIONS: Information derived from or of value to NASA activities. Publications include conference proceedings, monographs, data compilations, handbooks, sourcebooks, and special bibliographies.

TECHNOLOGY UTILIZATION PUBLICATIONS: Information on technology used by NASA that may be of particular interest in commercial and other non-aerospace applications. Publications include Tech Briefs, Technology Utilization Reports and Technology Surveys.

Details on the availability of these publications may be obtained from:

SCIENTIFIC AND TECHNICAL INFORMATION OFFICE

NATIONAL AERONAUTICS AND SPACE ADMINISTRATION

Washington, D.C. 20546